Master thesis

Development of the Detector Control System for the Muon Forward Tracker at ALICE

Hiroshima University, Graduate School of Science,
Department of Physical Science, Quark Physics Laboratory
M154616
Kosei Yamakawa

Supervisor : Associate Professor Kenta Shigaki
Chief Examiner : Associate Professor Kenta Shigaki
Vice-Examiner : Associate Professor Kenichi Ishikawa

February 24, 2017

Abstract

We have been performing the ALICE experiment to study the nature of the quark-gluon plasma, which is a new state of matter expected by Quantum ChromoDynamics, and to understand quark confinement and chiral-symmetry restoration, which is considered as the origin of hadron mass. After several years of data taking, we defined an upgrade program of ALICE for the LHC Runs 3 and 4. One part of this program is the Muon Forward Tracker (MFT). The MFT should improve the invariant mass resolution and measurement of heavy flavors down to low transverse momenta at the forward pseudo-rapidity.

I am interested in the physics brought by the MFT, but the LHC Run 3 will start only in 2021. I, therefore, decided to contribute to the MFT installation and operation by development of the Detector Control System (DCS). The DCS, also called a slow control, is responsible for the safe and reliable operation of the experiment. First, I have designed the general architecture of the MFT DCS. The MFT DCS is composed of SCADA systems and communication protocols as the software components and power supply systems, readout electronics such as First Level Processor and Readout Units, a cooling system, and sensors including thermometers and anemometers as the hardware components. Then, I have set up a test system which has 2 nodes, a worker node and an operator node as a small MFT. Two commercial SCADA systems named WinCC OA run on the nodes, and they are connected by distributed projects of WinCC OA. In addition, WinCC OA includes OPC and Distributed Information Management system (DIM) as communication protocols which are needed to communicate between WinCC OA and either readout electronics or other PC ' s. The worker node has an Embedded Local Monitoring Board (ELMB) and thermometers, a Pt100 and an NTC thermistor. The worker node is also connected with a PC, which reads out a silicon pixel detector named pALPIDE, via ethernet. Using the test system, I can monitor the temperature of pALPIDE via DIM and the air temperature via OPC with the ELMB. Also, I can operate the ELMB, and the test system works well as the small MFT. I will have completed the MFT DCS in 2018 and will install it in 2019.

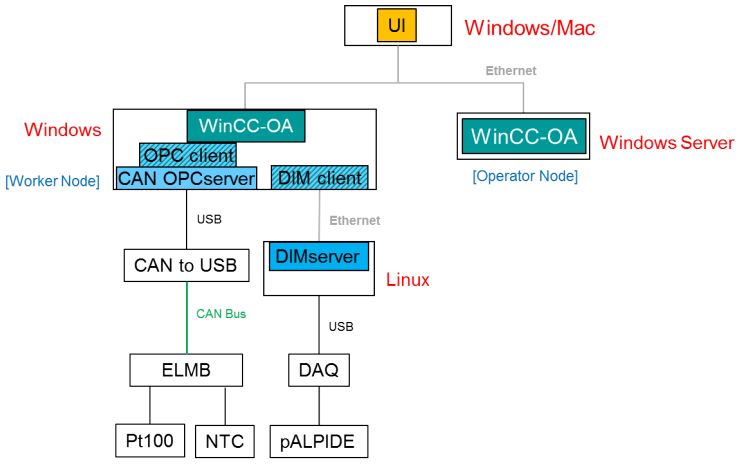

Figure: Architecture of the Test System

Contents

List of Figures

List of Tables

1 Introduction

1.1 Quark-Gluon Plasma

Quantum ChromoDynamics (QCD) is a theory to discriminate behaviours of quarks and gluons. Due to the feature of QCD, namely asymptotic freedom, we cannot take out quarks and gluons alone from hadrons at ordinary environment. However, QCD calculations expect quarks and gluons move freely in an extreme high temperature and dense matter (Fig. 1). The heated and dense medium is a new state of matters, and we call the matter Quark-Gluon Plasma (QGP).

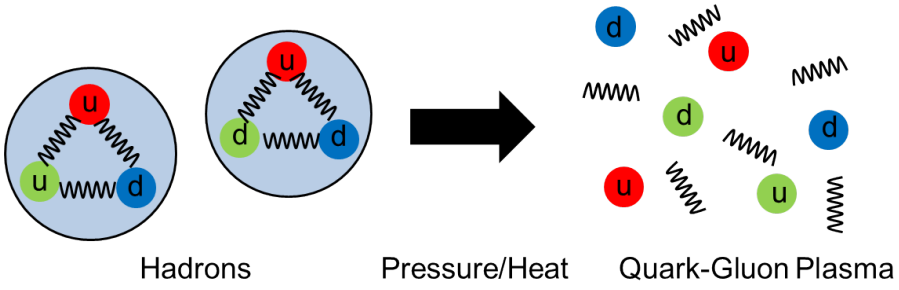

Figure 1: Schematic generation mechanism of the QGP

There are predictions that critical temperature for phase transition is around 200 MeV ($\sim 2 \times 10^{12}$ K) and the QGP existed at ten micro-seconds from the Big Bang (Fig. 2). Thus, our recognitions of characters of the QGP lead to our knowledges of the early universe. Ultra relativistic heavy ion collision experiment is the only generation method of the QGP.

1.2 Research Background

We have been performing A Large Ion Collider Experiment (ALICE) to study the nature of QCD and the QGP with the Large Hadron Collider (LHC). There are theories predict signatures and examinations of the QCD matter, like J/ψ suppression and strangeness production. For example, the J/ψ suppression, the effective temperature, and the anisotropic flow, the ALICE collaboration has reported as the probes of the QCD medium . However, there remain several essential questions such as the nature of quark confinement and chiral symmetry restoration, which we consider as the origin of light quark mass. For further experimental study of QCD and the dense medium, our needs are high resolution in the transverse momentum and the invariant mass.

Then, we project an upgrade programme of the ALICE equipment in the LHC Long Shutdown 2 (LS2) from 2019 to the end of 2020 towards Run 3 from 2021 and Run 4 from 2026 [2]. The Inner Tracking System, the Muon Forward Tracker, the Time Projection Chamber, the Fast Interaction Trigger, and the computing system are our major targets of the upgrade plan. Due to precise measurement of low transverse momentum particles with high resolution by the upgrade, we will be able to challenge the questions above.

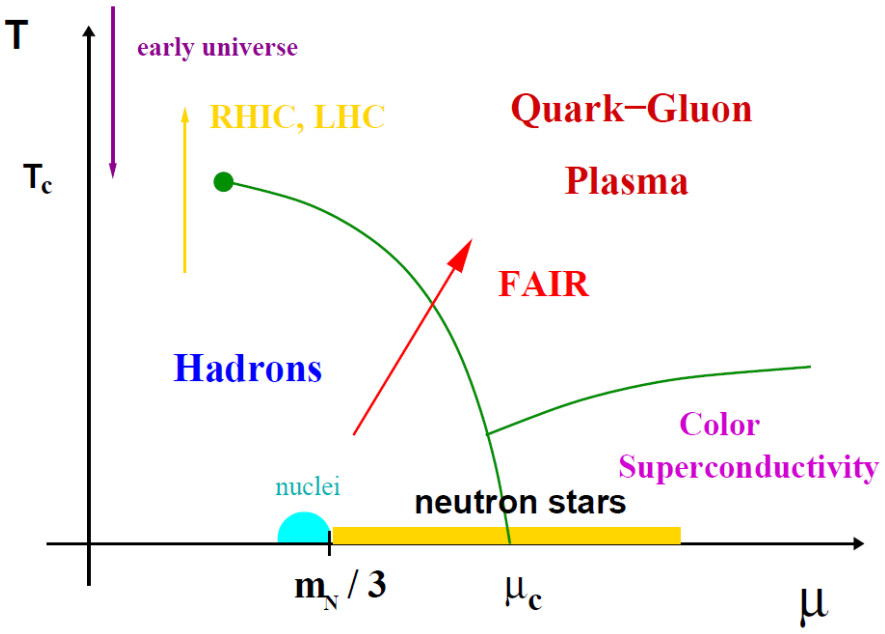

Figure 2: QCD phase diagram [1]

1.3 Object of my study

Physics with the upgraded ALICE detectors, in particular with the Muon Forward Tracker (MFT), after LS2 is my interest. For example, in-medium energy loss mechanism of heavy flavours and chiral symmetry restoration in low mass dimuon. However, the MFT is production stage at present, and Run 3 data taking will start in 2021, hence I cannot analyse physics with the MFT now. I, therefore, decided to contribute to the MFT installation and operation by development of the Detector Control System (DCS) for physics I am interested in.

First, I have to arrange an architecture of the MFT DCS. For the purpose, I have summarized a document for a hardware and software structure of the MFT DCS. The document shows the number and the installation location of all the components used in the MFT control system. The design document follows the form provided by the ALICE DCS team. Also, I have set up a test system as a mini MFT with devices and software used in the current ALICE DCS. Thanks to the test system, I can learn technique for the development and installation of the DCS.

2 ALICE Upgrade Program

2.1 Overview

The aims of the ALICE experiment, which is focusing on the heavy ion collisions experiment only in four major LHC experiments (ALICE, ATLAS, CMS, and LHCb), are understanding of the nature of QCD, the properties of the QGP, and the origin of hadrons' masses. The results of Run 1 revealed that the limitations of the current ALICE detectors prevent us from the precise measurement, especially in the low transverse momentum (p_{T}) region and the low invariant mass part [3]. Also, the LHC accelerator group plans to increase the beam interaction rate up to 50 kHz and the beam luminosity of $L = 6 \times 10^{27}\mathrm{cm}^{-2}\mathrm{s}^{-1}$ in Pb-Pb collisions after the LHC LS2. The proposed collision rate in the LHC Run 3 is a few times larger than the present readout rate of the ALICE equipment. Therefore, we decided an upgrade programme of the ALICE apparatuses including the detectors and the computing system to further experimental study (Fig. 3). There are other upgrades of readout electronics of Transition Radiation Detector (TRD), Time Of Flight (TOF), PHoton Spectrometer (PHOS), and Muon spectrometer.

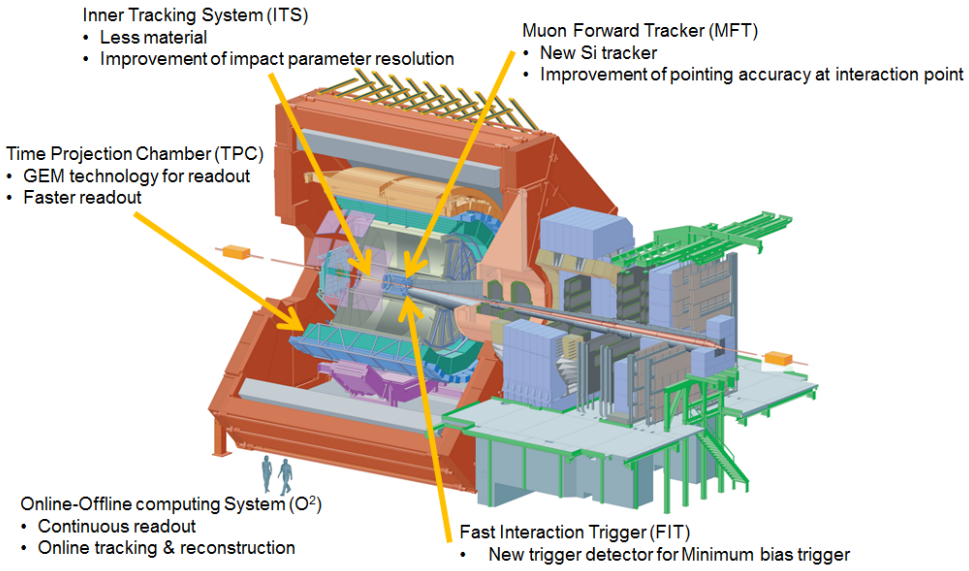

Figure 3: Overview of the ALICE major upgrade

2.2 Physics Motivation

Precise measurements of heavy flavour production, quarkonia production, and dileptons, mainly in low p_{T} region in Run 3 are our plans. I show the physics motivation of the ALICE upgrade.

- Quarkonia

  In general, quarkonia, in particular J/ψ, are good probes of the QGP. Nonetheless, our difficulty of explanation of suppression pattern of ψ(2S) re-

quires other models. There are the statistical hadronization model and the kinetic transport model as proposed models.

The statistical model considers charm quarks thermalize in the dense QCD matter and hodronize at chemical freeze out. The amount of charm quarks is a key parameter of this statistical theory, hence we must measure the production cross section of charm quarks with high precision to test this theoretical model. On the other hand, the kinetic transport model proposes recombination of charm quarks in the QGP as charm quarks production mechanism. The production yields and elliptic flow are crucial observables for testing the kinetic model.

- Heavy Flavours

  There are two major topics, which are thermalization and energy loss mechanism in the QGP, related to heavy quarks measurement. These topics are particularly close each other.

  In the current understanding, heavy flavours lose their energy in the dense medium, and they thermalize participate in the elliptic flow. Actually, we have measured the non zero flow of D meson. However, the energy loss mechanism of heavy quarks is not known well. Theories propose collisional energy loss and radiative energy loss are the mechanisms of quarks in the QCD matter. Also, they consider partons lose their energy by radiative mechanism, in other words gluons radiation, mainly.

- Dileptons

  There is a QCD prediction that the chiral symmetry breaking is the origin of hadrons. The theoretical prediction is that there is the chiral symmetry restoration in the high temperature matter, hence the masses of light vector mesons, especially ρ meson, shift lower mass. For lower mass shift observation, we need high resolution in the low invariant mass region.

  We consider the spectrum of real direct photon is a probe of the source temperature. By measurement of dileptons at $0.15 < M_{\rm ee} < 0.3$ GeV/c^2 and $p_{\rm T} > 1$ GeV/c, we can measure the direct photon spectrum as the QGP temperature.

Table 1 shows the comparison of the current physics reach and the proposed physics reach.

2.3 Detector Upgrade

Here, I introduce the overview of the important detector upgrades.

2.3.1 Inner Tracking System

The Inner Tracking System (ITS) covering the central pseudo-rapidity is a detector for tracking and particle identification (PID) of charged particles in Runs 1 and 2. There are the six layers, the two Silicon Pixel Detectors (SPD), the two Silicon Drift Detector (SDD) and the two Silicon Strip Detectors (SSD) from the most inner layer. The impact parameter accuracy of the ITS is enough for the production measurement of charm mesons at $p_{\rm T} > 1$ GeV/c. However, the performance of the present system is short for the precise measurement of them

Table 1: Comparison of the physics current reach and the proposed physics reach [3].

Observable	Approved		Upgrade	
	$p_{\mathrm{T}}^{\mathrm{Amin}}$ (GeV/c)	statistical uncertainty	$p_{\mathrm{T}}^{\mathrm{Umin}}$ (GeV/c)	statistical uncertainty
Heavy Flavour				
D meson R_{AA}	1	10 % at $p_{\mathrm{T}}^{\mathrm{Amin}}$	0	0.3 % at $p_{\mathrm{T}}^{\mathrm{Amin}}$
D meson from B decays R_{AA}	3	30 % at $p_{\mathrm{T}}^{\mathrm{Amin}}$	2	1 % at $p_{\mathrm{T}}^{\mathrm{Amin}}$
D meson elliptic flow	1	50 % at $p_{\mathrm{T}}^{\mathrm{Amin}}$	0	2.5 % at $p_{\mathrm{T}}^{\mathrm{Amin}}$
D meson from B elliptic flow	not accessible		2	20 % at $p_{\mathrm{T}}^{\mathrm{Umin}}$
Charm baryon-to-meson ratio	not accessible		2	15 % at $p_{\mathrm{T}}^{\mathrm{Umin}}$
$\mathrm{D_s}$ meson R_{AA}	4	15 % at $p_{\mathrm{T}}^{\mathrm{Amin}}$	1	1 % at $p_{\mathrm{T}}^{\mathrm{Amin}}$
Charmonia				
J/ψ R_{AA} (forward rapidity)	0	1 % at 1 GeV/c	0	0.3 % at 1 GeV/c
J/ψ R_{AA} (mid rapidity)	0	5 % at 1 GeV/c	0	0.5 % at 1 GeV/c
J/ψ elliptic flow	0	15 % at 2 GeV/c	0	5 % at 2 GeV/c
ψ(2S) yield	0	30 %	0	10 %
Dielectrons				
Temperature (intermediate mass)	not accessible			10 %
Elliptic flow	not accessible			10 %
Low-mass spectral function	not accessible		0.3	20 %
Heavy Nuclear States				
Hyper(anti)nuclei ${}^{4}_{\Lambda}\mathrm{H}$ yield	35 %			3.5 %
Hyper(anti)nuclei ${}^{4}_{\Lambda\Lambda}\mathrm{H}$ yield	not accessible			20 %

at lower p_{T}, because the proper decay length of the charm baryons ($\sim 60\mu$m) is shorter than the impact parameter resolution of the ITS [7]. The capability of the current apparatus prevents us to study beauty mesons and hadrons for the same reason. In addition, the readout rate of 1 kHz in nucleus-nucleus collisions causes of the above problems.

The main subject of the ITS upgrade is improvements of the impact parameter resolution and tracking performance by material budget reduction. To reduce material budget, we will use Monolithic Active Pixel Sensors (MAPS) in the ITS detectors. Thus, the impact parameter resolution of the new ITS will increase as shown in Fig. 4. Moreover, the readout rate also will increase up to 100 kHz in Pb-Pb collisions and up to 400 kHz in pp collisions. Three Inner Barrel layers (IB) and four Outer Barrel layers (OB) compose the upgraded ITS, and the OB separates into two middle layers and two outer layers (Fig. 5).

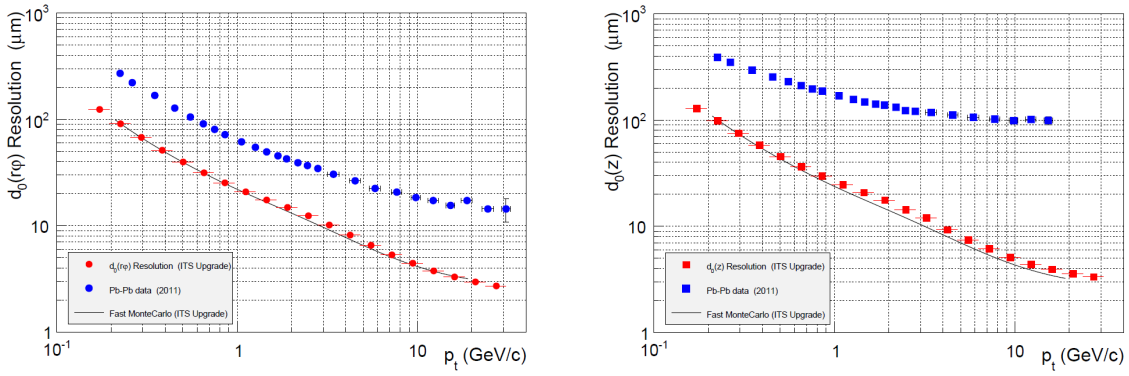

Impact parameter resolution in transverse plane

Impact parameter resolution in longitudinal plane

Figure 4: Comparison of impact parameter resolution with the current ITS (blue) and with the new ITS (red) [7]

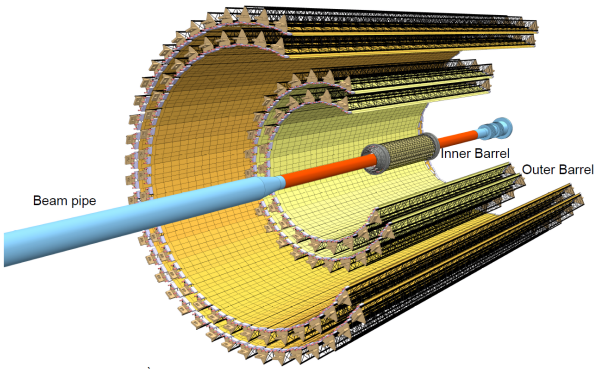

Figure 5: Layout of the new ITS [7]

2.3.2 Muon Forward Tracker

The Muon spectrometer of ALICE covers at the forward pseudo-rapidity of $2.5 < \eta < 4$ (Fig. 6). The main object of the spectrometer muons tracking, and we have studied the quarkonia

production, the open heavy flavours production and the low mass dimuons with the detector. However, the multiple scattering of muons in the front absorber causes inaccuracy of the interaction points, accordingly the current equipment cannot show the full potential. For example, it is difficult for us to reject muons coming from semi-muonic decays of pions and kaons at low p_{T} and to distinguish prompt and displaced J/ψ production.

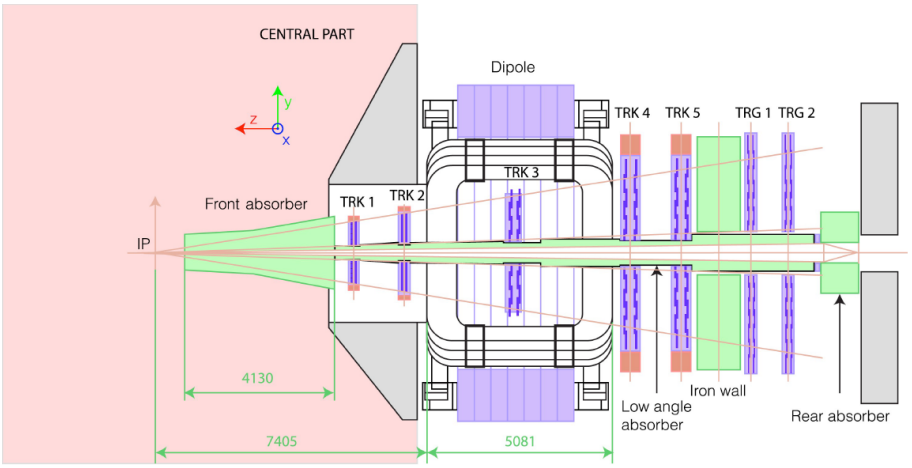

Figure 6: Layout of the current Muon system [4]

To solve the problem, we suggested the Muon Forward Tracker (MFT) in the upgrade programme. The strategy of the MFT is that the MFT disks will track charged particle from an interaction point before incoming the front absorber [4]. I will show the details of the MFT project in Section 3.

2.3.3 Time Projection Chamber

A Time Projection Chamber (TPC) is a detector for charged particles tracking and PID. The information from the TPC plays an important role at ALICE and will provides key observables in the proposed programme. Besides, readout systems of the current TPC are Multi-Wire Proportional Chamber (MWPC) based readout chambers. The operation mode of the existing TPC readout chambers is Gating Grid mode, which prevents back-drifting ions from the amplification region of a MWPC to enter the drifting volume. However, the gated operation of the MWPC based readout systems effects the limitation of the readout rate of 3.5 kHz.

For TPC operation at 50 kHz, we will replace MWPC based chambers with Gas Electron Multiplier (GEM) based readout systems. We can operate the GEM system with continuous readout at a collision rate of 50 kHz, thus we will be able to analyse physics observables we could not access previously. Fig. 8 shows a comparison the assumed $e^{+}e^{-}$ invariant mass spectra with the current TPC and with the upgraded TPC in Pb-Pb collisions at $\sqrt{s_{\mathrm{NN}}} = 5.5$ TeV. Furthermore, the estimated number of recorded events with the improved TPC is about two orders of magnitude more than that of events with the present TPC in a typical yearly heavy ion run of about 3 nb^{-1}.

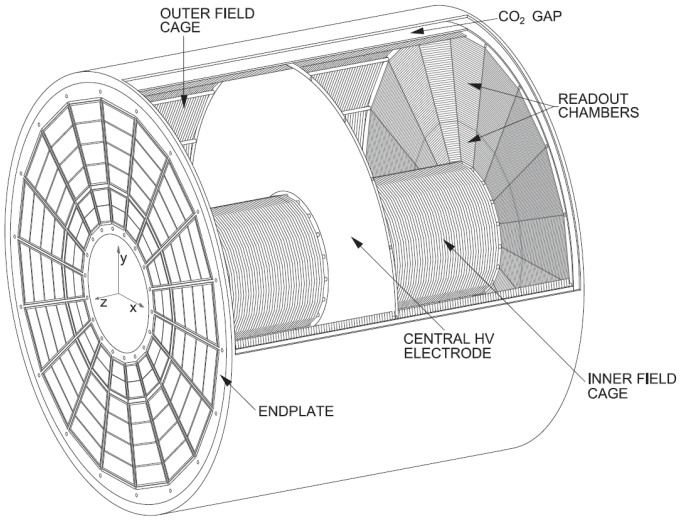

Figure 7: Layout of the TPC [8]

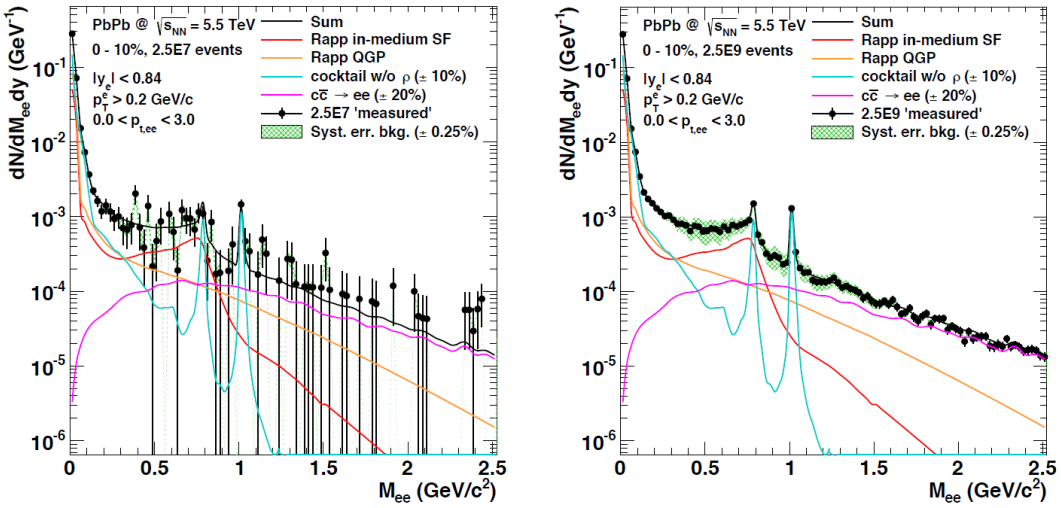

Figure 8: Comparison the assumed spectra with the current TPC (left panel) and with the new TPC (right panel) [8]

2.3.4 Fast Interaction Trigger

There are three forward detectors, the T0, V0, and Forward Multiplicity Detector (FMD), at ALICE. We have used them for minimum bias trigger, multiplicity trigger, beam-gas rejection, collisions time for Time Of Flight (TOF) detector, offline multiplicity and event plane determination. Following the increase of collision rate, we plan to displace the current forward detectors with the Fast Interaction Trigger (FIT). Technologies used in the FIT are advances of the T0 and V0 detectors. The new trigger detector meets the requirements such as the followings:

- Minimum bias trigger
- Event multiplicity determination for either central or semi-central collision selection and triggering
- Time resolution better than 50 ps

Fig. 9 shows the comparison of the present trigger detector and the new trigger detector.

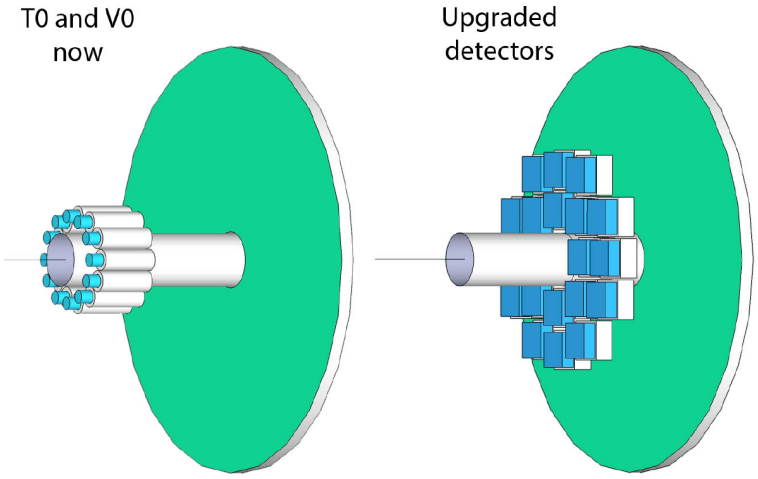

Figure 9: Comparison of the current trigger detector (left) and the upgraded trigger detector (right) [9].

2.4 Computing System Upgrade

2.4.1 Online-Offline computing system

The data taking scenario in the LHC Run 3 is continuous readout with minimum-bias trigger in Pb-Pb collisions at 50 kHz and in pp and p-Pb collisions at 200 kHz. Therefore, the predicted data amount of Run 3 will be 3.4 TB/s and about 100 times larger than that of Run 1. To process larger volume data immediately, we propose the Online-Offline computing system (O^2) [6].

The O^2 system collects raw data and performs the detector calibration and the data reconstruction partially to compress the volume of data in parallel (Fig. 10). The First Level Processors (FLPs) and the Event Processing Nodes (EPNs) are the new computing devices for data collection and data volume reduction. The FLPs reads the raw data from

the detectors via GBT links, and they decrease the data volume by zero cluster finder and baseline collection. The EPNs receive the data from the FLPs, and the EPNs squeeze the data amount by online tracking and reconstruction for each detector. Only reconstructed data are carried in the storage. The O^2 also provides the framework which we need for simulation and analysis.

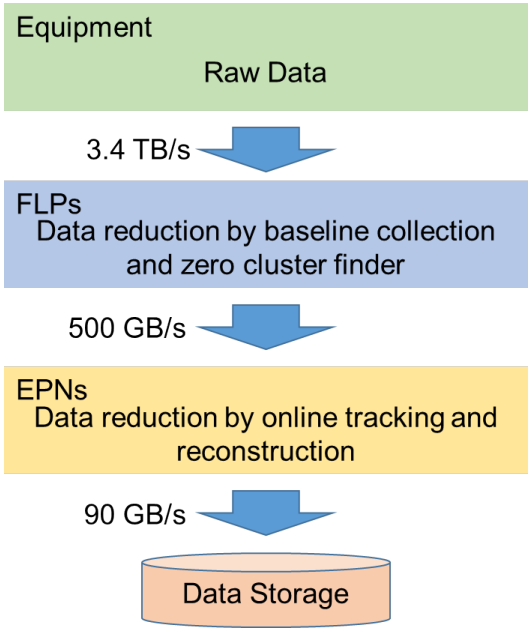

Figure 10: Flow structure of O^2 computing system

3 Muon Forward Tracker

3.1 Overview

The results of the ALICE Run 1 declared that the multiple scattering of muon in the hadron absorber affected muon spectra larger than the estimations. The Muon spectrometer provided us the large interaction point in Run 1, thus we cannot study the low mass dimuon production and heavy flavours production precisely, especially in the low p_{T} region. In the same reason, we have measured the production cross section of inclusive muons from c and b quarks from lower limited p_{T}. To overcome the problems, we plan to install the MFT.

The main subject of the MFT is an improvement of an accuracy of an interaction point. To achieve this purpose, the location of the MFT detector is between the absorber and interaction point. As a result, the MFT can track charged particles before coming into the absorber (Fig. 11).

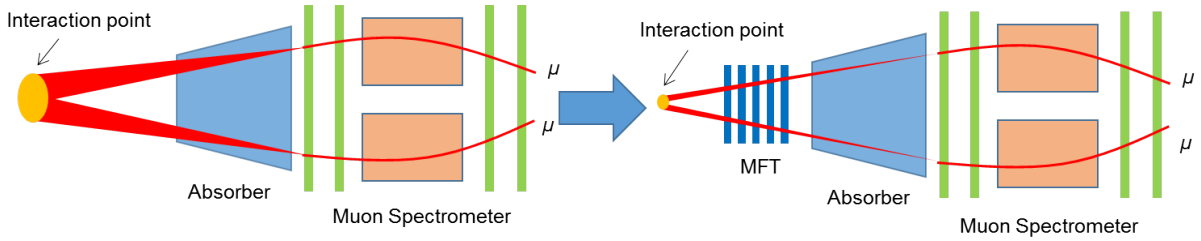

Figure 11: Strategy of improvement of accuracy with the MFT

The MFT covers the pseudo-rapidity range of $-3.6 < \eta < -2.45$. That range is smaller than the pseudo-rapidity region of the Muon spectrometer of $-4 < \eta < -2.5$, because of the beam pipe.

3.2 Physics Program in Pb-Pb collisions

Thanks to the MFT installation, we will be able to analyse the physics that we cannot study before the Run 3. Our physics motivations with the MFT and the Muon spectrometer are measurements of open heavy quarks, quarkonia, and low mass dimuons in heavy-ion collisions. I will introduce the physics programme of the MFT in heavy-ion collisions, and Table 2 presents the comparisons of the current and the suggested observables.

- Quarkonia

  In order to measure the production of prompt J/ψ, we need to remove the information of the QGP and b hadrons decay J/ψ. For the goal, we need to separate prompt and non-prompt J/ψ.

  We have measured inclusive J/ψ R_{AA} at forward rapidity in lead-lead collisions at $\sqrt{s_{\mathrm{NN}}} = 2.76$ TeV (Fig. 12) [10]. The result is consistent that of CMS in the high p_{T} region, but R_{AA} measured at PHENIX is more suppressed compared to ALICE's result in low transverse momentum. In the transport models, charm quarks recombination in dense matter generates about half amount of J/ψ in the low p_{T} region.

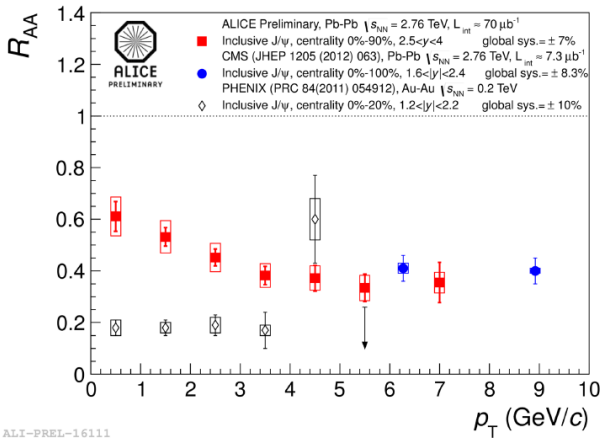

Figure 12: Measured inclusive J/ψ production at forward pseudo-rapidity [10]

Also, we have measured elliptic flow of inclusive J/ψ in Pb-Pb collisions at $\sqrt{s_{\rm NN}} = 2.76$ TeV, the data are consistent with two transport models (Fig. 13) [10]. The models include J/ψ regeneration about 30 % of the measured J/ψ. In addition, the theoretical calculations drawn in full line and dash-dotted line count J/ψ from b hadrons decay . There are few differences between these calculations. To explain the J/ψ generation models, we need to take more precision data for accuracy measurement.

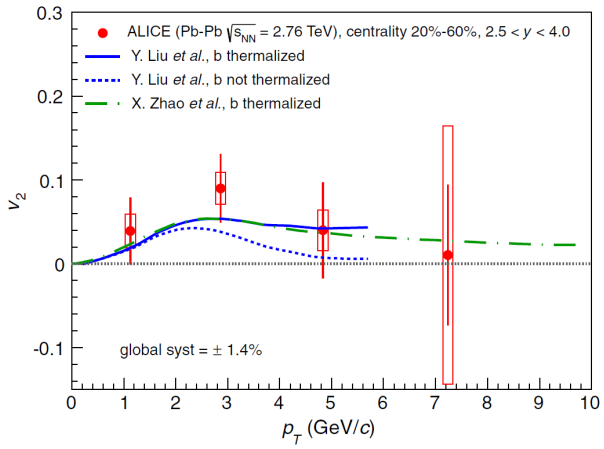

Figure 13: Measured J/ψ elliptic flow at forward rapidity [11]

Moreover, the MFT will provide a possibility that we measure the ψ(2s) production and its $R_{\rm AA}$ as a function of $p_{\rm T}$. The production mechanism of ψ' will test the statistical hadronisation model.

Besides, we plan to measure the bottomonium production such as Υ(1S) down to $p_{\rm T}$ of 0 GeV/c. ATLAS and CMS have reported Upsilon production measurement. However, the muon $p_{\rm T}$ threshold of 3 GeV/c makes harder measurement in low $p_{\rm T}$ region at ATLAS and CMS. Measurement of Upsilon production in the low transverse momentum part is an important subject.

- Open Heavy Flavours

  The MFT will allow us to detach charm and bottom quarks. Because of disentanglement of heavy flavours, we will improve the understanding of the energy loss mechanism of heavy quarks in the dense QCD matter with the MFT.

  We still don't understand the energy loss mechanism of charm and beauty quarks in the dense medium well. Theoretical prediction of parton energy loss mechanisms is there are radiative energy loss and collisional energy loss. Also, theorists predict Landau-Pomeranchuk-Migdal effect or dead cone effect, however no experiment explores the energy loss mechanism.

  The other motivation is elliptic flow. It seems to us that v_2 gives information of collective expansion and thermalization of heavy flavours in the dense medium at $p_{\mathrm{T}} <$ 2-3 GeV/c. Flow at 3 GeV/$c < p_{\mathrm{T}} <$ 6 GeV/c is a sensitive recombination process of heavy quarks. Furthermore, flow at $p_{\mathrm{T}} >$ 6 GeV/c suppresses the path length dependence of parton energy loss in the QGP.

  We have reported inclusive muons R_{AA} and v_2 from heavy quarks hadron at forward pseudo-rapidity (Fig. 14). We have been able to measure only R_{AA} above transverse momentum region of 4 GeV/c and v_2 above transverse momentum range of 3 GeV/c, hence it is difficult for us to compare our results and the theories. Therefore, it is necessary that precise measurements of in-medium energy loss of heavy quarks to test the theories.

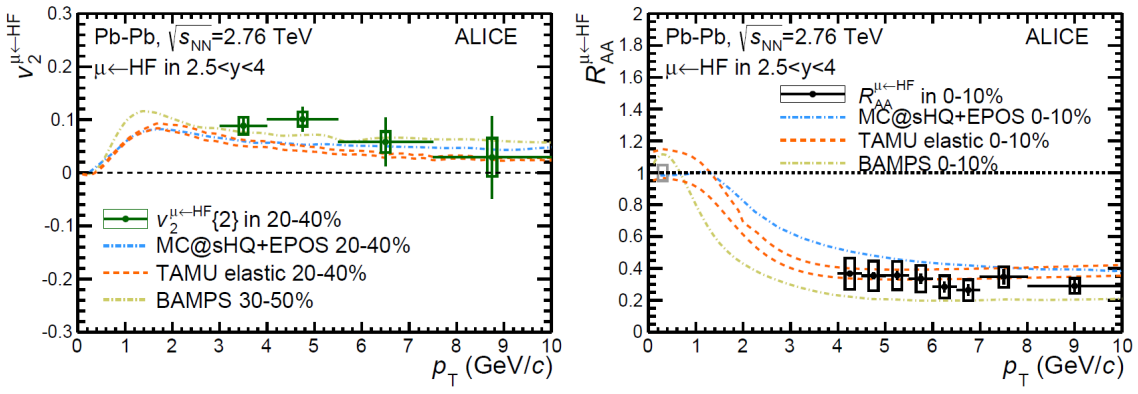

Figure 14: Elliptic Flow (left panel) and nuclear modification factor (right panel) of muons from heavy flavour hadrons decay in central Pb-Pb collisions [12]

- Low mass dimuons

  The MFT should improve the resolution of the low mass dimuon spectrum and the signal over background ratio compared to that with only the Muon spectrometer (Fig. 15). We will be able to challenge the important problems of QCD with the MFT.

  There is a theoretical prediction that there is chiral symmetry restoration, which we believe as the origin of hadrons, in the high temperature matter. However, no experiment has observed the chiral symmetry restoration.

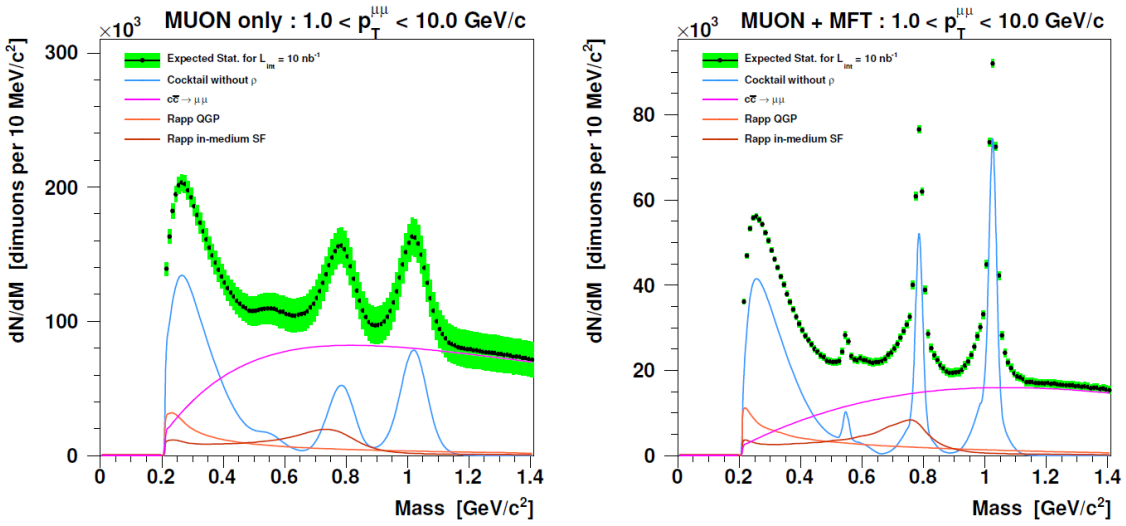

Left panel: Dimuon spectrum with only the Muon spectrometer
Right panel: Dimuon spectrum with the MFT and the Muon spectrometer

Figure 15: Comparison between the expected low mass spectra without the MFT (MUON) and with the MFT (MUON + MFT) in central collisions [4]

Similarly, we can measure the temperature of QGP using dimuon invariant mass and p_{T} spectra. It appears that dileptons in the invariant mass spectrum at 1.5-2.5 GeV/c^2 come from thermal radiation at the early stage of the QGP. Production process of virtual photons is same that of real photons, hence we can assume virtual photon spectrum using the extrapolation of the dilepton measurement in the low or intermediate mass regions.

3.3 Hardware Components of the MFT detector

The MFT detector consists of two half MFTs, an upper half and a lower half, and both of the half MFTs are the same structure. The half MFT is composed of a Power Supply Unit (PSU) and five half disks. A half disk is divided into two half planes, a front side and a back side. Three half disks, numbered 0, 1 and 2, have ladders, also, two half disks, numbered 3 and 4, have ladders, DC-DC converters and GBT-SCAs each. The PSU comprises DC-DC converters and GBT-SCAs, since half disks 0, 1 and 2 are too limited to have them. Then, a zone is a cluster of ladders, for example, a zone of half disk 0 consists three ladders, and voltages are applied zone by zone. A ladder consists of ALICE Pixel DEtector (ALPIDE) chips. Figure 11 shows the components of the MFT, and Table 3 presents the total amount of the MFT components.

Table 2: Comparison of the current reach with the Muon spectrometer (MUON) and the proposed upgrade with the Muon spectrometer and the MFT (MUON + MFT). Assuming integrated luminosity is 10nb^{-1} in central nucleus-nucleus collisions. [4]

Observable	MUON only		MUON + MFT	
	$p_{\mathrm{T}}^{\mathrm{min}}$ (GeV/c)	uncertainty	$p_{\mathrm{T}}^{\mathrm{min}}$ (GeV/c)	uncertainty
Inclusive J/ψ R_{AA}	0	5 % at 1 GeV/c	0	5 % at 1 GeV/c
ψ' R_{AA}	0	30 % at 1 GeV/c	0	10 % at 1 GeV/c
Prompt J/ψ R_{AA}		not accessible	0	10 % at 1 GeV/c
J/ψ from b-hadrons		not accessible	0	10 % at 1 GeV/c
Open charm in single μ			1	7 % at 1 GeV/c
Open beauty in single μ			2	10 % at 2 GeV/c
Open HF in single μ no c/b separation	4	30 % at 4 GeV/c		
Low mass spectral func. and QGP radiation		not accessible	1-2	20 % at 1 GeV/c

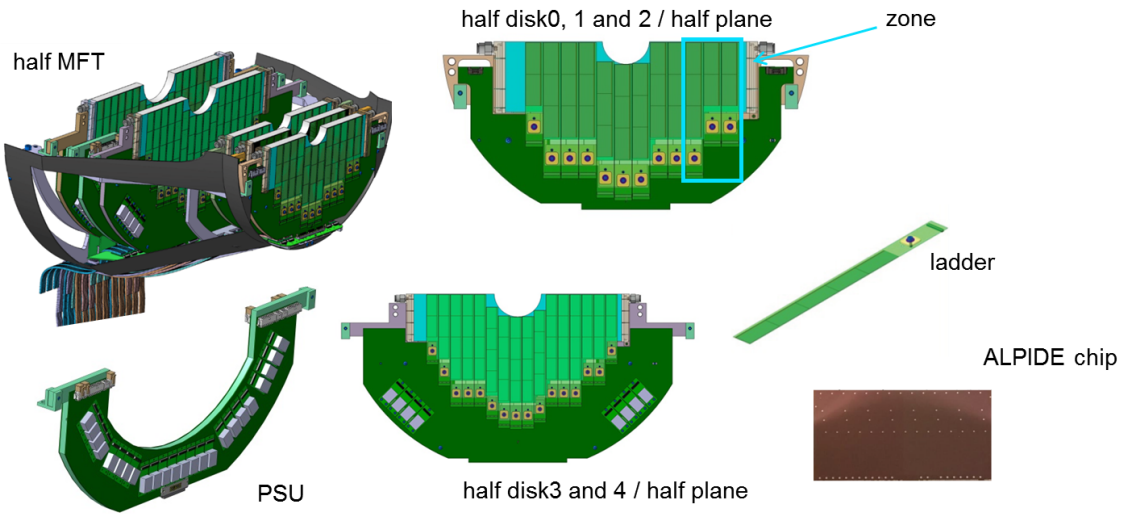

Figure 16: The MFT components

Table 3: MFT Components [5]

Item	Total Amount
MFT	1
Half MFT	2
Half Disk	10
PSU	2
Half Plane	20
Zone	80
Ladder	280
Chip	920

4 Detector Control System at ALICE

4.1 Overview of the Detector Control System at ALICE

There are the ALICE detectors in the cave at about 50 meters underground and we cannot go there due to radioactivity during collisions. No one can come to the cavern, therefore, we must operate and monitor the experimental equipment remotely. The Detector Control System (DCS), also called slow control, allows us to control and supervise the experimental apparatuses from the ALICE control room at LHC Point2. For example, we can configure the applied voltage of detectors and monitor the status of them with the DCS. Also, when a temperature of a device is higher than the expected working temperature, a finite state machine or an interlock system will stop the detector. In other words, the DCS is responsible for safe and reliable operation of the experiment.

The DCS consists of three layers which are the supervision layer, the process management layer and the field management layer (Figure 17). The supervision layer is in the ALICE control room, and it has graphical user interfaces provided by SCADA systems. The process management layer is in the counting room between the control room and the cavern, and it consists of computing systems, including SCADA system and communication protocols such as OPC and DIM. Also, controllers such as Programmable Logic Controllers (PLCs) and power supply systems are included in the process management layer. SCADA systems connect the supervision layer and the process management layer via ethernet. Buses called USB or CANbus connect the computing systems in the process management layer and controllers or Power Supply systems (PSs). Then, the field management layer is in the cave, and it is composed of field buses, nodes, sensors, and readout electronics. The field management layer also contains detector setups. Cables for power supply system connect the equipment and the PSs, and cables such as GBT link (see Section 4.3.6) connect the readout electronics and either controllers or readout electronics.

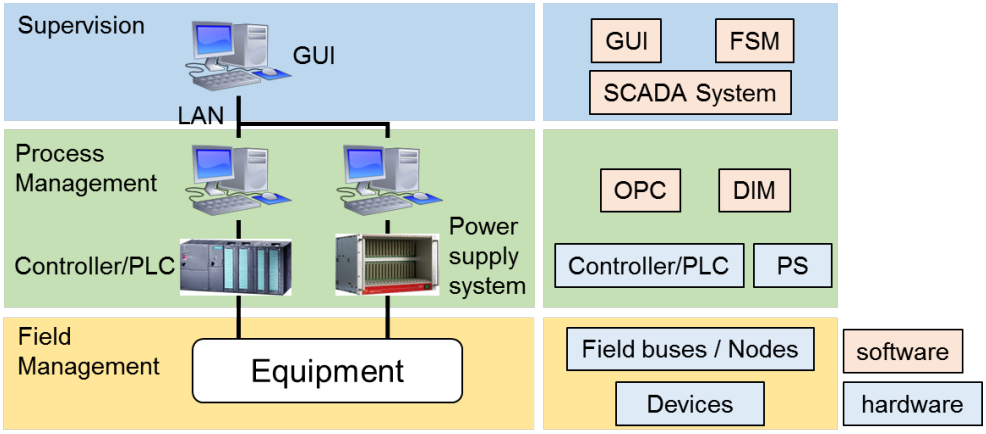

Figure 17: Architecture of DCS

4.2 DCS Software

4.2.1 SCADA system and WinCC OA

Supervisory Control And Data Acquisition (SCADA) system is one of the industrial control systems and used for system operation and process monitoring [13]. Experts in the fields of power plants, manufacturing lines and system for the prevention of disasters use the SCADA systems. WinCC Open Architecture (WinCC OA) is one of the commercial SCADA system manufactured by ETM.

There are six components on WinCC OA as follows [14];

- Runtime database

  Data from devices are saved in the runtime database. We can visualize and process them by accessing the database.

- Archive

  WinCC OA users can store the data in the runtime database for a long time and extract by the user interface and other processes.

- Alarm generation & handling

  When some kind of error which is defined by DCS experts happen, WiCC OA will generate alarms. Alarms are archived in an alarm database, and displayed on an alarm display.

- Graphical editor

  Thanks to graphical editor, we can build graphical user interfaces and other panels.

- Scripting language

  A scripting language named CTRL (called control) is used in WinCC OA, and it allows us to handle the data which are in the database from graphical user interfaces.

- Graphical parametrization tool

  Owing to graphical parametrization tool, we can define the structure of the database and select the data which should be stored and etc.

There are the event manager (EVM), the database manager (DBM), user interface manager (UIM), control manager (Ctrl), Application Programming Interface manager (API), and drivers (D) as the WinCC OA components (Figure 18).

The responsibility for all communication inter-managers of WinCC OA lies with the event manager, and the event manager gets data from any drivers. The database manager supplies the interface to the database. User interface manager can receive the data from the database and send the data to the database to be sent to the device, they can also request to keep an open connection to the database and be informed (for example to update the screen) when new data arrive from the devices. Any data processing is provided by the Ctrl managers as background processes, by running a scripting language. The language is like C with extensions. Users can their own programs in C++ using the API manager to access the data in the database. Drivers provide the interface to the devices to be controlled. These can be WinCC OA provided drivers like Profibus, OPC, and so on.

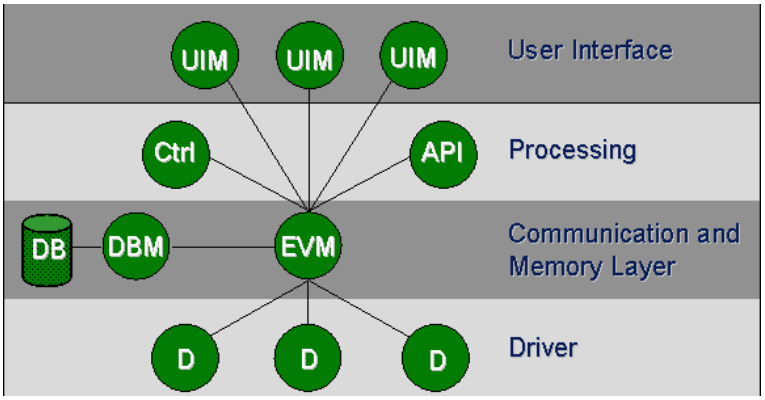

Figure 18: Architecture of WinCC OA [14]

There are a few features of WinCC OA. First, we can run WinCC OA on multi platform, Windows and Linux. Second, WinCC OA is openness; for instance, developers can write own programs in C++. Third, there are distributed systems which enable us to link many stand-alone systems via network on WinCC OA (Figure 19). Because of the above reasons, CERN selects it. Four LHC experiments, fixed target experiments such as COMPASS and NA60, the LHC accelerator group, the electrical network group and cooling & ventilation group use WinCC OA.

On WinCC OA, values are treated as Data Point Elements (DPEs), and they are used to configure FSM and user interface panels. Data Point Type (DPT) is a data structure of a device , and users define the DPT format in accordance with the equipment. The left panel of Fig. 20 presents a DPT of HvChannel. Data Point (DP) is a hierarchy defined by DPT. The right panel of Fig. 20 shows an DPs example of HvChannel. The HvChannel DPT contains two DPs named Channel1 and Channel2. The DPEs of Channel1 are v0, state, vMon, and so on. Other files such as common and original are configuration file of the DPEs.

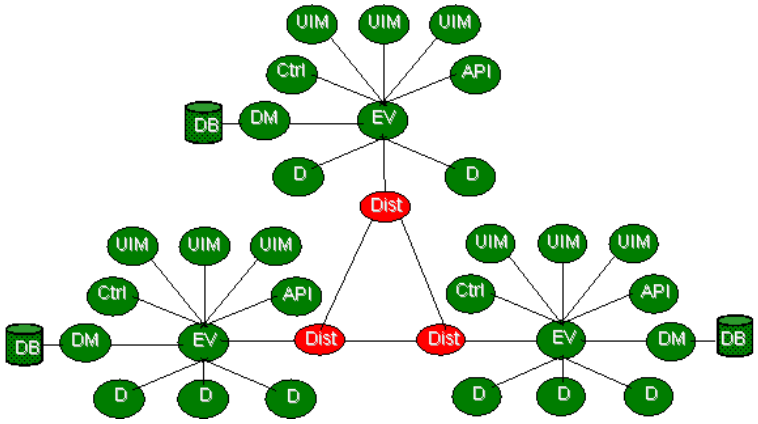

Figure 19: Distributed systems in WinCC OA [14]

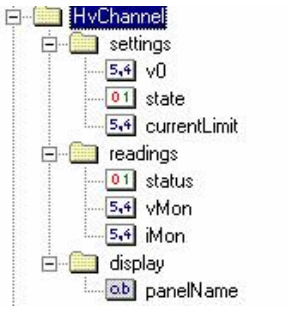

Example architecture of a Data Point Type

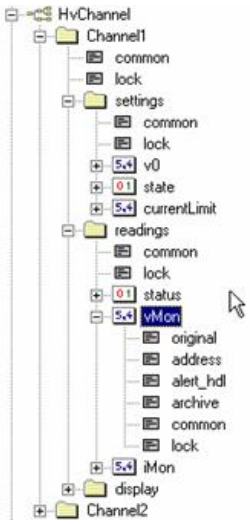

The example architecture of Data Point

Figure 20: Data Point Data Point Element [14]

4.2.2 Joint Control Project Framework

For reduction of the cost and manpower for developing control systems in four LHC experiments, CERN IT/CO group has developed Joint COntrol Project Framework (JCOP Fw) [15]. This framework is based on WinCC OA projects, and it runs on WinCC OA only. Using JCOP Fw, users can operate CAEN power supplies, Embedded Local Monitor Board (ELMB) and other devices.

The DCS experts use the following tools, mainly;

- Device Editor and Navigator

  Device Editor and Navigator is a main interface of JCOP Fw. Users can configure and operate the devices using it. In addition, it includes configuration of finite state machines.

- Trending Tool

  When users monitor temperatures and humidity, trending tool visualize the parameters.

- DIM Manager

  DIM is a CERN's original communication protocol, and it is one of the most important parts of the DCS architecture. The DIM manager provides a DIM client to exchange data with a server,thus users can set the data as DPs.

- Component Installer

  Since JCOP Fw is a CERN's unique framework, DCS experts need to install JCOP Fw on WinCC OA. The users can choose frameworks which users want to install with the installer.

Figure 21 shows the framework software components. In this figure, PVSS mean a SCADA system, and it is former WinCC OA.

4.2.3 OPC

OPC is the standard for safe and trusted exchange of data in industrial automation and other fields [16]. A lot of commercial devices employ OPC protocol, for example power supply systems produced by CAEN. To use OPC communication, the OPC foundation which is responsible for the development and maintenance of this standard must certificate devices which users will use.

There are two specifications in the OPC standard, the OPC Classic and the OPC Unified Architecture (OPC UA). The OPC Classic is separated into three specifications, the OPC Data Access (OPC DA), the OPC Alarms & Events (OPC AE), and the OPC Historical Data Access (OPC HDA).

- OPC DA

  The OPC DA specification defines the exchange of values, time and quality. General activities of the OPC DA are update of data which includes parameters of time and quality.

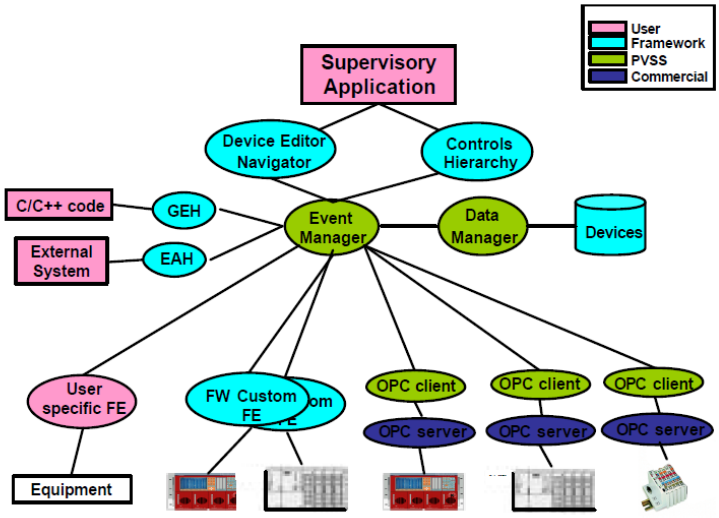

Figure 21: JCOP framework software components[15]

- OPC AE

  The OPC AE specification characterizes the exchange of state values, state management, alarms and event types.

- OPC HDA

  The OPC HDA specification defines the methods to historical data and timed-stamp data.

- OPC UA

  The OPC UA is unified of all OPC Classic specifications.

In the current DCS, we use the OPC DA for communication, however, the ALICE DCS team plan to use the OPC UA from the Run 3.

For the OPC communication, DCS experts need devices which are certificated by the OPC foundation, and PC which has an OPC server and OPC clients such as WinCC OA (Figure 22). OPC clients do not access to devices for getting data directly, but they get data via OPC server. OPC servers are published by manufactures which produce devices users will use.

4.2.4 Distributed Information Management system

Distributed Information Management system (DIM) is a communication protocol as same as OPC, and CERN produced it [18]. DIM consists of servers, clients, and DIM Name Servers (DNSs) (Figure 22).

Servers and clients exchange “services”, and a service is a set of data which are any type or size. Servers register the services to a name server, and servers publish services to clients. By asking a name server at startup, clients subscribe to services, furthermore servers publish and update the services automatically either at regular times or the condition change. Then,

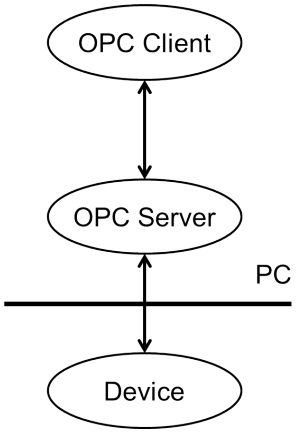

Figure 22: Architecture of OPC communication

users can operate the equipment which is connected to a PC which has a DIM server via a DIM client.

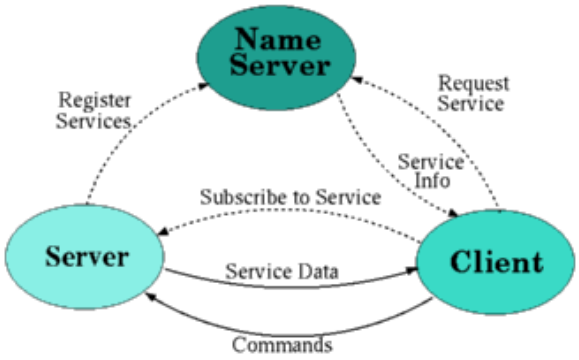

Figure 23: Architecture of DIM[18]

OPC is a reliable communication protocol, however, devices need the OPC foundation certifications. On the other hand, DIM is a CERN's original communication protocol and free for use. Therefore, DIM is used for communication between WinCC OA and handmade devices mainly.

4.3 DCS Hardware

4.3.1 FRontEnd Device servers

For DCS communication, the ALICE DCS group will install FRontEnd Device servers (FREDs) in the counting room [21]. FREDs receive DCS commands from WinCC OA and translates them to the native language of CRUs and forwards them to ALFs. In addition, they receive data from ALF and send them to WinCC OA.

4.3.2 First Level Processor

First Level processors (FLPs) will be computing nodes and collect data from detectors at a rate of 3.4 TB/s. FLPs will compress the data, including DCS data from detectors by a factor of six and send physics data to Event Processing Nodes (EPNs). FLPs and FREDs will communicate with each other via network (Fig. 24)

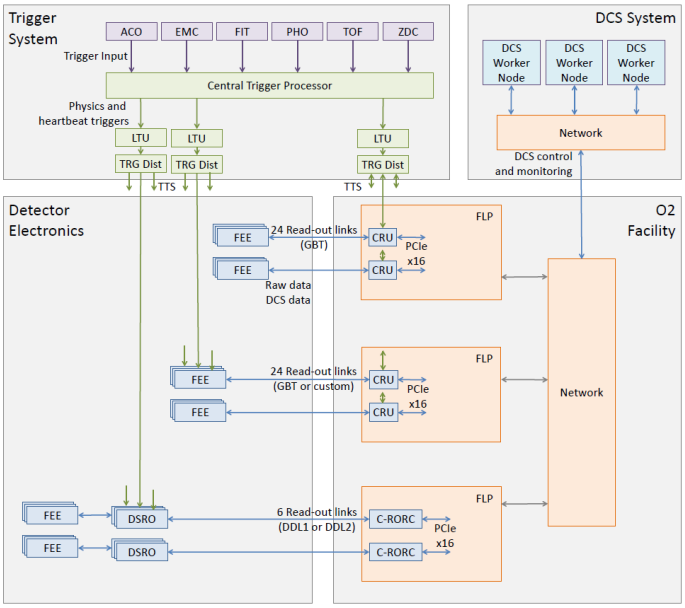

Figure 24: Diagram of the O^2[6]

4.3.3 ALICE Low-level Frontend Interface

ALICE Low-level Frontend (ALF) will be an interface and enable us to access to the readout cards and detectors, also its lightweight server will run on the FLPs. Due to ALFs, we can read and write registers and monitor thorough regularly published data on WinCC OA. FREDs and ALFs will communicate directly for sending DCS commands and DCS data each other.

4.3.4 Common Readout Unit

Common Readout Unit (CRU) is an interface on an FLP between detector readout electronics and DCS electronics which are ALF and FRED. Field Programmable Gate Array (FPGA) is the base of the CRUs, thus experts can develop CRUs detector specific. For reduction of the size of data, CRUs will perform clustering and background subtraction. As for the MFT DCS, CRUs will strip the data stream from ALPIDEs which will include physics data and their status such as temperature and applied voltage. CRUs will communicate front-end electronics of detectors via GBT links.

4.3.5 Embedded Local Monitoring Board

For the purposes of the detector control and monitoring, the ATLAS experiment developed Embedded Local Monitoring Boards (ELMBs) [19].It can be put on the frontend electronics

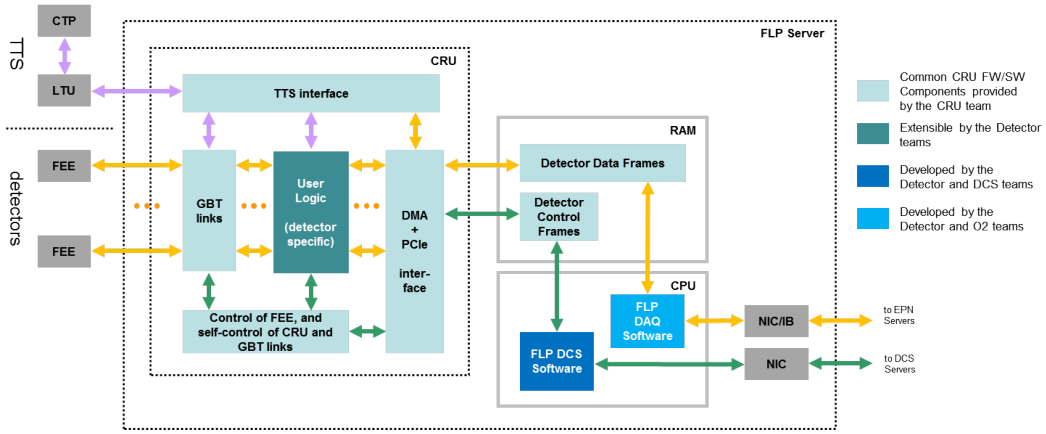

Figure 25: Diagram of CRU[22]

or a general purpose motherboard.

The block diagram of the ELMB is shown in Figure 26. There are 18 general purpose I/O, 8 digital inputs and 8 digital outputs on the ELMB. It can also have 16 bit ADC and multiplexing for 64 analog inputs optionally.

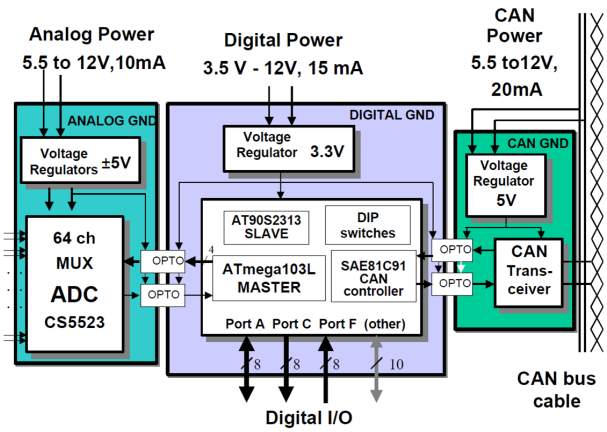

Figure 26: Block diagram of ELMB[19]

The ELMB on an mother board is powered via CAN and needs power of 20 mA at 5.5 V. Also, the ELMBs and PCs are connected by CAN-bus, but PCs which do not have CAN-bus ports need a CAN to USB modules.

4.3.6 Giga-Bit Transceiver Project and Components

It is said that particle physics will avail enormous amount of data transmitted from experimental equipment at high luminosity. To deal the data, we will require readout electronics which have wide bandwidth compared with the current. Also, they are going to be required to be radiation-tolerant. As for ALICE, it is expected that the amount of readout data of Run 3 will be about 100 times larger than those of Run 1. The Giga-Bit Transceiver (GBT) project has started to produce components that satisfy these requirements [23].

Figure 27 shows the concept of GBT. There are four components, a trans-impedance amplifier (GBTIA), a laser driver (GBTLD), a transceiver (GBTX) and a slow control adapter (GBT-SCA). Mean of "Slow Control" in Figure 27 is same that of the DCS.

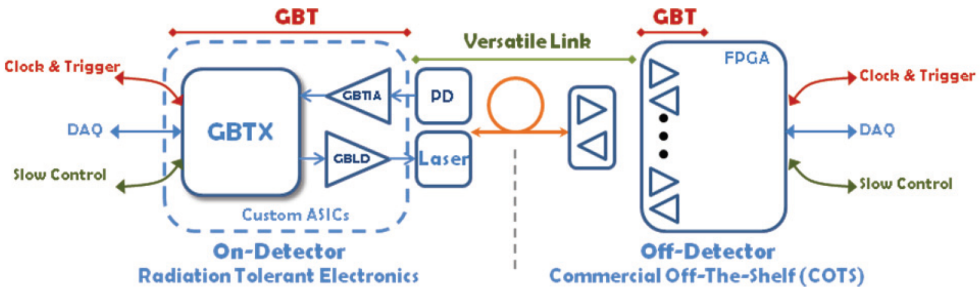

Figure 27: Flow structure of GBT[23]

Here, I introduce the components needed for the development of the DCS.

- GBTX

  The GBTX is a flexible link interface chip and responsible for high speed bidirectional optical link, and its bandwidth is 3.2 - 4.8 Gb/s [24]. It manages the communication between in the counting room receiver and transmitter and the front end module on detectors. For Timing and Trigger Control, Data Acquisition (DAQ), and Slow Control, the GBTX provides three paths, and a single optical link combines these paths as shown in Figure 27. Thanks to the GBTX, we will be able to avail readout data, trigger data, timing control distribution, slow control, and monitoring simultaneously.

- GBT-SCA

  The GBT-SCA is an ASIC for detector operation and their environmental monitoring. On the GBTX, the GBT-SCA connects to e-port by bidirectional link, called e-link, and e-link runs at 40 MHz double data rate mode, giving an effective data rate of 80 Mbps [25].

  Figure 28 shows the block diagram of the GBT-SCA. There are 1 I^2C masters, 1 SPI master, 1 JTAG master, 32 general I/O as bidirectional interface ports, and it also includes 31 analog inputs multiplexed to 12 bit ADC and 4 analog outputs controlled by 4 independent 8 bit DACs on the GBT-SCA.

4.3.7 Readout Unit and Board

The MFT readout electronics is composed of the Readout Units (RUs) for the connected pixel sensors control and monitoring and receive data [26]. The RU board has FPGAs, GBTXs, and a GBT-SCA to interface with ALICE O^2 and with the central trigger processor via GBT links, and the board process all detector data including physics data and DCS data (Fig. 29). The RUs will be located at about 5 meters distant from the MFT, and cables manufactured by Twinax connect the RU boards and the MFT.

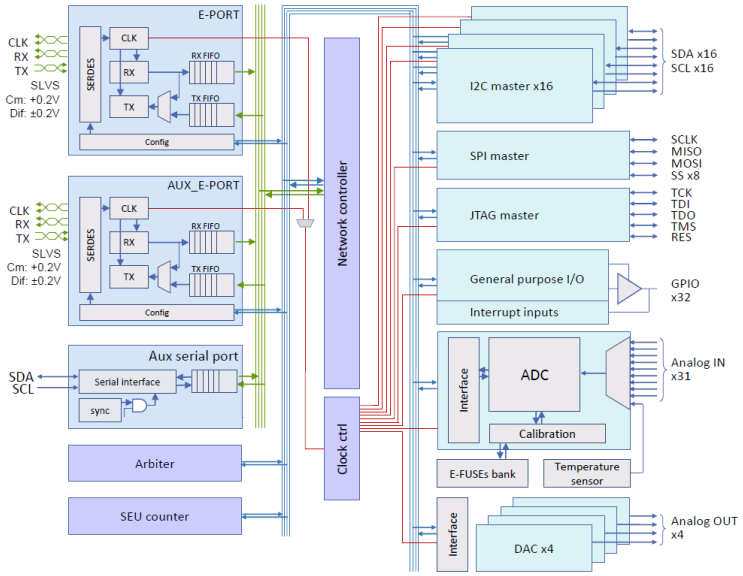

Figure 28: GBT-SCA block diagram[25]

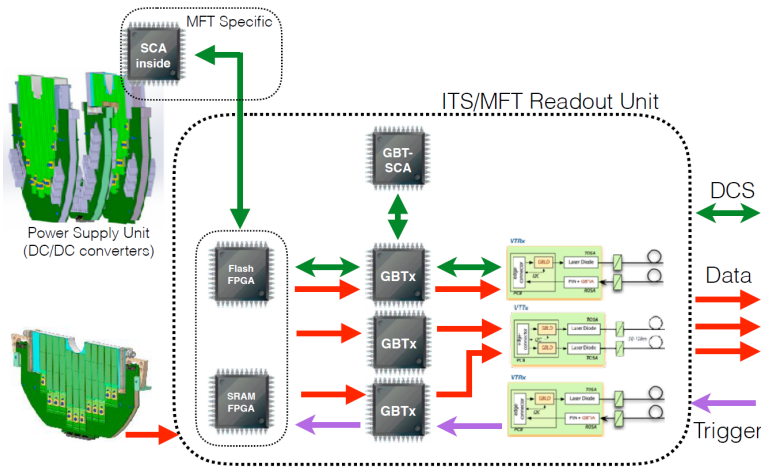

Figure 29: The architecture of Readout Unit[27]

4.4 Flow Structure of DCS Data in ALICE Run 3

The DCS archives the data in the DCS database after each period of collisions, called run, for offline analysis in Runs 1 and 2 [21]. In Run 3, the O^2 project plans to take and process data simultaneously, therefore, the DCS needs to send about 100,000 values to FLPs in 20 ms time frames.

The O^2 includes the DCS as a part of the project. Therefore, the ALICE DCS needs the electronics meet requirement of the O^2, the FRED and the ALF. DCS data, commands and status, are translated into CRUs' language for smooth shipping with them. Figure 30 shows the data flow structure of the DCS. The words "control" mean DCS data, including DCS commands, and "Data stream" include physics data and the status of detectors.

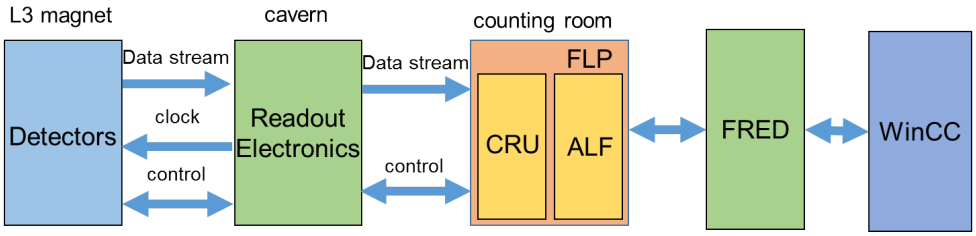

Figure 30: Structure of DCS data flow

5 Design of the MFT DCS and Test System

5.1 Hardware Architecture

The three layers compose the MFT DCS as same as the ALICE DCS. The supervision layer consists of only a part of power supply unit. The process management layer contains four worker nodes, an operator node, power supply system, and the O^2 and DCS electronics. The field management layer has GBT-SCAs, RU crates, RU boards, DC-DC converters, Low Drop Out (LDO) regulators, ALPIDEs, and thermometers. LDO regulator plays a role as same as a DC-DC converter, but we call LDO regulator which has small difference between input voltage and output voltage. Fig. 31 shows the general architecture of the MFT DCS. I followed the explanation of the detector drawing (Fig. 32) to make the diagram.

In Fig. 31, the left node shows the power supply systems for DC-DC converters and LDOs. The DC-DC converters supplies the power the zones, and the LDO regulators supply the bias voltage to ALPIDEs. Low Voltage (LV) means voltages for the silicon pixel chips in the field of high energy physics. We will operate the CAEN family as the LV power supply system (Table 4). We can control the EASY systems only via A1676A branch controllers (Fig. 33). We will use LDO regulators of MIC39152 manufactured by Micrel for bias voltages of ALPIDEs. Also, we will handle DC-DC converters of DC-DC module FEASTMP CLP from CERN.

Table 4: The lists of CAEN supplies we will use[5]

Model	Type	Description
SY4527	Crate	Universal multichannel power supply system
A1676A	Controller	Branch controller for the EASY system
A3486	Power Supply	48V power supply for the EASY system
EASY3000	Crate	Magnetic field and radiation tolerant crate for hostile area
A3009	Board	12 channel 8 V / 9 A / 45 W power supply board
A2519	Board	8 channel 15V/5 A (50 W) individual floating channel board

The second left means a power supply system for five RU crate and eighty RU boards. However, the system is not defined, so “PS” means power supply are written. The second from right works for control and monitoring of ALPIDEs, DC-DC converters, LDOs and their temperatures via RUs.

The right node is a cooling system. We will use Programmable Logic Controllers (PLCs) produced by SIEMENS as cooling plant controllers.

5.1.1 Serial Bus Setting for Regulators Monitoring and Control

From the GBT-SCAs, we will configure and monitor DC-DC converters and LDOs. Table 5 shows the list of serial buses on the GBT-SCA for monitoring and control.

On the CRUs, data from the ALPIDEs are stripped into physics data and DCS data. Therefore, we design to read the status of ALPIDEs from CRUs.

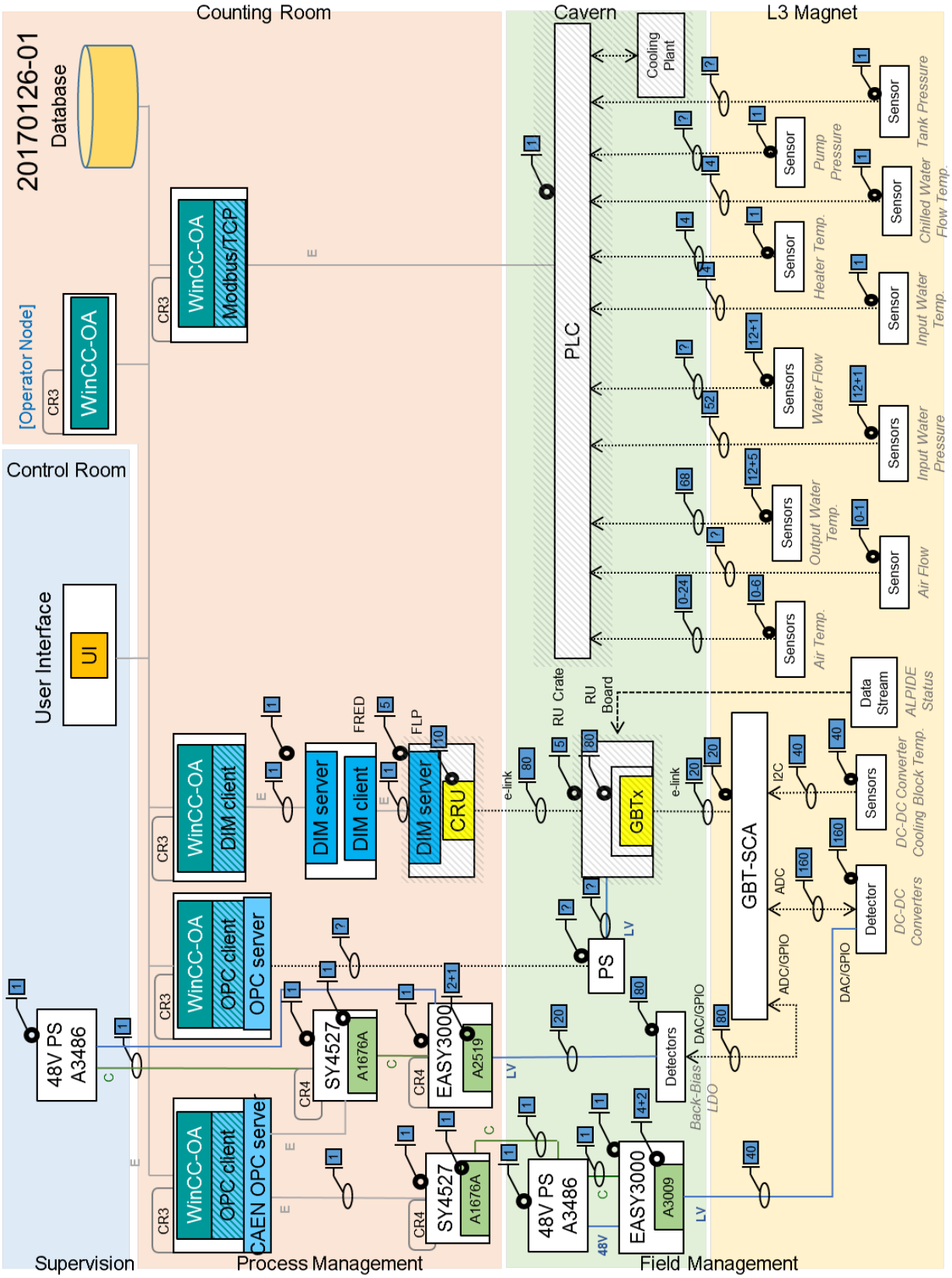

Figure 31: Architecture of the MFT DCS

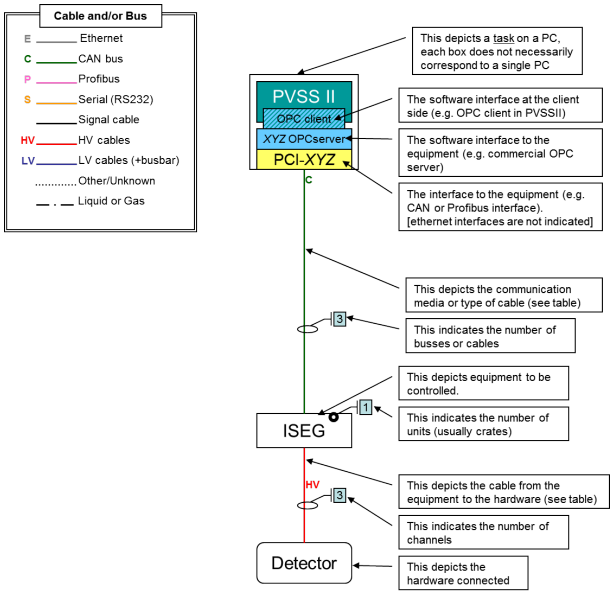

Figure 32: Explanation of the detector drawings, field layer

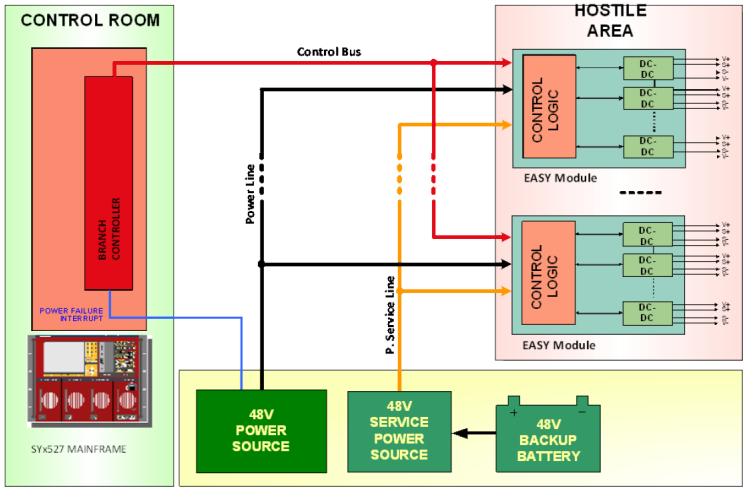

Figure 33: CAEN system diagram [28]

Table 5: List of the serial buses for control and monitoring

Device	Serial Bus
DC-DC Converters' ON/OFF	I/O
DC-DC Converters' applied voltage monitoring	ADC
Cooling Block Temperature	I^2C

5.1.2 Options for Readout Electronics

There are two options for the readout electronics of the MFT DCS. One is with GBT-SCAs, and the other is with ELMBs.

Option A GBT-SCA

> As I mentioned earlier, the GBT-SCAs are new devices for the DCS from CERN. The O^2 systems need that adapters. Therefore, I take into consideration as a primary solution. However, the GBT project team is developing it, so I cannot test a test system with a GBT-SCA.

Option B ELMB

> The ELMB is a traditional device for the DCS, and we have used them for the current ALICE DCS. Therefore, I take into consideration it as a backup solution of the MFT DCS.

5.2 Software Architecture

The software architecture of the MFT DCS consists of two layers, the supervision layer and the process management layer. There is a user interface in the supervision layer. An operator node and four worker nodes compose the process management layer. WinCC OA runs on all of them, and WinCC OA on the operator node provides the user interface. The worker node for the LV supply has CAEN OPC server, and the worker node for the RU power supply has the OPC server produced by a manufacture which produces power supply system we will use. The worker node for the equipment control and monitoring will communicate with FRED via DIM. FSM will run on the operator node.

5.3 Test System

I have set up a test system with an ELMB as a small MFT. The system includes almost needed skills for the MFT DCS with the ELMBs. I will show the architecture of the test system and results.

5.3.1 Test System Architecture and Components

The test system consists of an operator node, a worker node, and a user interface (Fig. 34). The worker node is a detector part of the small MFT, and the operator node is a computing part of it. WinCC OA runs on both of the nodes, and distributed projects of WinCC OA connect the nodes each other.

The worker node has the ELMB and two thermometers, a Pt100 and a Negative Temperature Coefficient (NTC) thermistor. Pt100 is a resistance thermometer, and NTC thermistor is a semiconductor thermometer. It is also connected to a Linux PC, which reads out a pALPIDE, via ethernet, and the OS is Cern CentOS 7 (CC7). WinCC OA on the worker node contains an OPC client and a DIM client. The worker node also has an OPC server to read out values from the ELMB. A DIM server and a DNS server run on CC7 for sending services to the DIM client and receiving commands from the client. Control and monitoring are done from the user interface, which is connected to the operator node via Windows Remote Desktop.

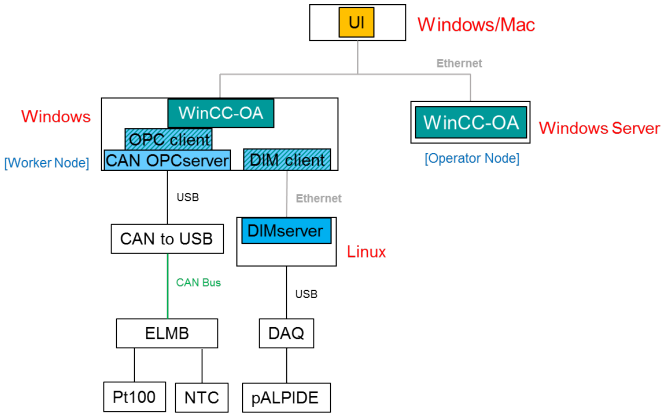

Figure 34: Architecture of the test system

5.3.2 Test System Setup and Results

First, I created the environment for the DCS with the ELMB. WinCC OA version of 3.11 was downloaded from the CERN engineering department page (https://wikis.web.cern.ch/wikis/display/EN/PVSS+Service+Download+3.11SP1), and installed it on the nodes. I made a distributed project on each node, and I confirmed that the nodes are connected each other (Fig. 35).

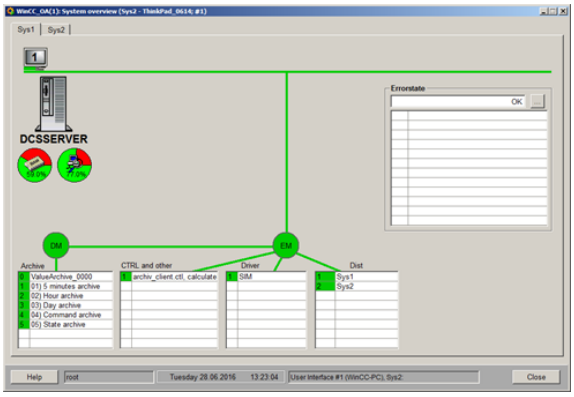

Distributed system panel on the operator node

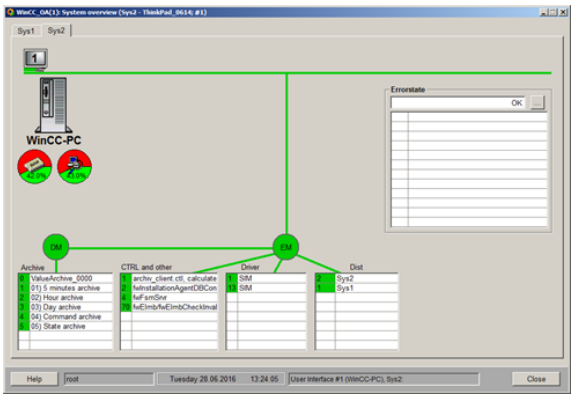

Distributed system panel on the worker node

Figure 35: Data Point Data Point Element

Next, I got the JCOP framework version 5.2.1 from CERN (https://wikis.web.cern.ch/wikis/display/EN/JCOP+Framework) and installed frameworks on both the worker node and the operator node using the installation panel. I selected the frameworks named AbalogDigital, BarGraph, Caen, ConfigurationDB, Core, DIM, FSM-ConfDB, Trending, and XML (Fig. 36). The right window in Fig 36 shows the installed framework components.

Next, I obtained a CAN OPC server and a JCOP framework component for the ELMB from the ATLAS ELMB Documentation and Framework Component page (https://twiki.cern.ch/twiki/bin/view/Atlas/DcsElmb). To use OPC, I wrote an OPC con-

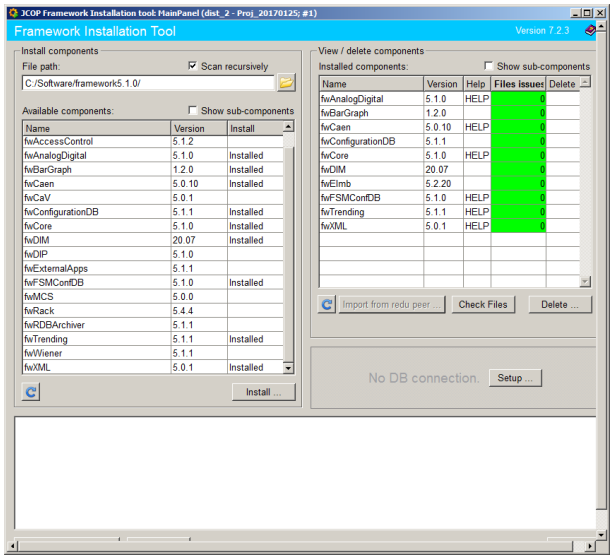

Figure 36: JCOP framework installation panel

figuration file as follows:

[CANBUS] CAN0 = KVCANServer+ 0 125000

[ELMB]
ELMB_1 = CAN0 1 NG

[ITEM]
CAN0.ELMB_1.PT_4W_0_1 =
(3.9083e-3-pow((1.5275e-5+2.31e-6*(1-CAN0.ELMB_1.ai_1*1000/(CAN0.ELMB_1.ai_0*100))),0.5))/1.1
6
CAN0.ELMB_1.NTC_4 = 1/(3.354016e-3+2.909670e-4*log(1.e-6*CAN0.ELMB_1.ai_4*1000000/2.5-
1.e-6*CAN0.ELMB_1.ai_4)/1000) +1.632136e-6*pow(log(1000000*1.e-6*CAN0.ELMB_1.ai_4/(2.5-
1.e-6*CAN0.ELMB_1.ai_4)/1000),2) +7.192200e-8*pow(log(1000000*1.e-6*CAN0.ELMB_1.ai_4/(2.5-
1.e-6*CAN0.ELMB_1.ai_4)/1000),3))-273.15

[INIT]
CAN0.NodeGuardInterval = 60000
CAN0.NMT = 1
CAN0.SyncInterval = 1000

In the configuration file, ELMB_1.ai_n ($n = 0, 1, 4$) mean analog input values from the Pt100 ($n = 0, 1$) and the NTC thermistor ($n = 4$).

I performed read out the temperature from the thermometers with the ELMB via OPC. I configured the temperatures as analogue input with the Device Editor and Navigator. Fig. 37 shows the temperature with the thermistor and the resistance thermometer. Red is the NTC thermistor measured temperature, and blue is the Pt100 measured temperature.

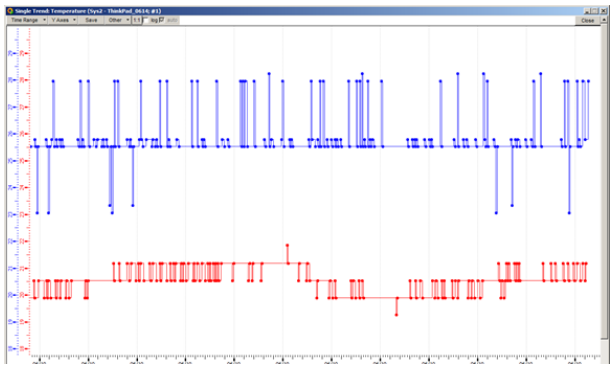

Figure 37: Temperatures of thermistors connected to the ELMB

For DIM communication, I added the DIM manager, named WCCOAdim, as following configuration (Fig. 38):

Options: -num 2 -dim_dns_node DELL_C221.hepl.hiroshima-u.acjp
Start mode: Manual

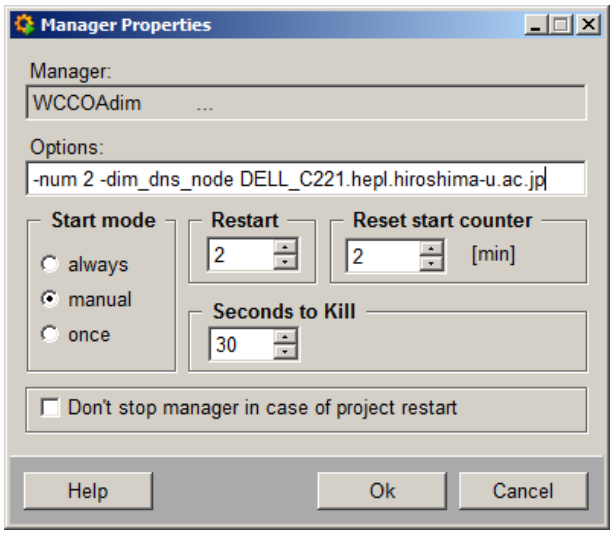

Figure 38: JCOP framework installation panel

JCOP DIM plays a role of a DIM client, so I don't need install DIM software on the worker node.

I downloaded a DIM software from the CERN DIM page (http://dim.web.cern.ch/dim/) and installed it on the CC7 for the DIM communication. I configured the name of DNS server as same as the CC7 host name "DELL_C221.hepl.hiroshima-u.ac.jp". Also, I set the DIM sever named "RUNServer" for pALPIDE temperature monitoring. DIM server sends the temperature to DIM client on the worker node.

I can also read the temperature of pALPIDE via DIM just like the thermometers via OPC. Fig. 40 presents the pALPIDE temperature on WinCC OA.

I have completed the test system as the small MFT with the ELMB and the pALPIDE.

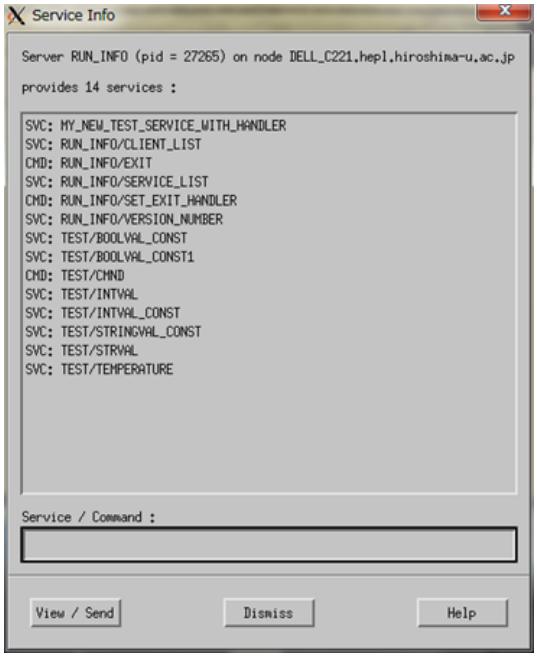

Figure 39: The list of services on RUNServer

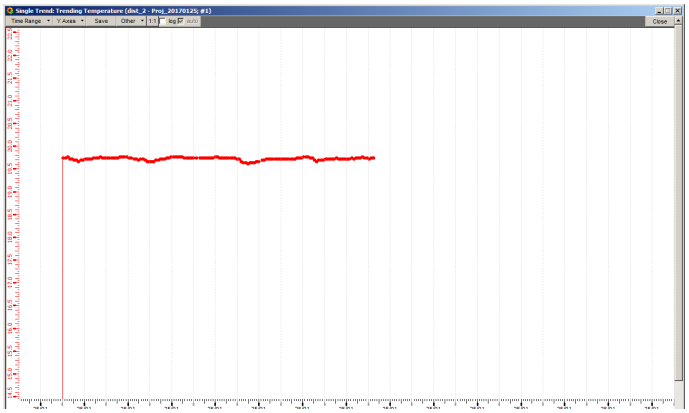

Figure 40: Temperature of the pALPIDE

6 Summary and Outlook

I have designed the general architecture of the MFT DCS. Mainly, I have summarised the number and the location of the MFT DCS items. Also, I have set up the test system, and the structure of the test system is as same as the current ALICE DCS.

In 2017 spring, prototypes of GBT-SCA and CRU will be completed and I will get them. Consequently I will install them in the test system, also I will try to read the pALPIDE status with them. By the end of 2017, I will install a ladder in the test system, and build the test bench at CERN. The plan of the MFT installation is in 2019, thus we need to complete before the MFT installation. Thus, I will complete the MFT DCS in 2018.

Acknowledgement

I would like to thank my supervisor and a convenor of the MFT work package 7 Associate professor K.Shigaki. He gave me the dissertation theme and advices for the architecture of the MFT DCS. I acknowledge all stuffs in Hiroshima University, Professor T.Sugitate, Assistant professor K.Homma, and Assistant professor T.Miyoshi for their useful comments. Also, I express my gratitude towards P.Chochula, O.Pinazza, and the other members of the ALICE DCS group. Not only they gave me helpful advices and comments, but also they lent me the ELMB setup for the test system. And I acknowledge K.Oyama for his practical opinions, including suggestions to points I did not pay attention to. I also thank A.Nobuhiro for his comments and help with pALPIDE readout, and I could not build the test without his advices.

References

[1] J. Schaffner-Bielich, Signals of the QCD Phase Transition in the Heavens, *Proceedings of Science*, CPOD07:062,2007

[2] Longer term LHC schedule, https://lhc-commissioning.web.cern.ch/lhc-commissioning/schedule/LHC-long-term.htm, accessed on 22 Dec, 2016

[3] B. Abelev *et al.*, Upgrade of the ALICE Experiment: Letter Of Intent, *J. Phys. G* 41 (2014) 087001

[4] ALICE Collaboration, Addendum of the Letter Of Intent for the Upgrade of the ALICE Experiment : The Muon Forward Tracker, CERN-LHCC-2013-014

[5] ALICE Collaboration, Technical Design Report for the Muon Forward Tracker, CERN-LHCC-2015-001

[6] ALICE Collaboration, Technical Design Report for the Upgrade of the Online-Offline Computing System, CERN-LHCC-2015-00

[7] ALICE Collaboration, Technical Design Report for the Upgrade of the ALICE Inner Tracking System, *J. Phys. G* 41 (2014) 087002

[8] ALICE Collaboration, Technical Design Report for the Upgrade of the ALICE Time Projection Chamber, CERN-LHCC-2013-020

[9] ALICE Collaboration, Upgrade of the ALICE Readout & Trigger System, CERN-LHCC-2013-019

[10] Christophe Suire for the ALICE Collaboration, Charmonia production in ALICE, *Nuclear Physics A* 910911 (2013) 106113

[11] ALICE Collaboration, J/Ψ Elliptic Flow in Pb-Pb Collisions at $\sqrt{s_{\rm NN}} = 2.76$ TeV, *Phys. Rev. Lett.* 111, 162301 (2013)

[12] ALICE Collaboration, Elliptic flow of muons from heavy-flavour decays at forward rapidity in Pb-Pb Collisions at $\sqrt{s_{NN}} = 2.16$ TeV, *Phys. Lett. B* 753 (2016) 41

[13] Softech, Development of SCADA, http://www.softech.co.jp/scada_main.htm

[14] The LHCb collaboration, PVSS Introduction for Newcomers, https://lhcb-online.web.cern.ch/lhcb-online/ecs/PVSSIntro.htm

[15] M. Gonzalez-Berges on behalf of the Framework Team, The Joint COntrols Project Framework, arXiv:physics/0305128

[16] OPC Foundation, https://opcfoundation.org

[17] CERN OPC Support , https://wikis.web.cern.ch/wikis/display/EN/OPC+Support

[18] C. Gaspar *et al.*, DIM, http://dim.web.cern.ch/dim/

[19] B. Hallgren *et al.*, The Embedded Local Monitor Board (ELMB) in the LHC Front-end I/O Control System, 7th Workshop on Electronics for LHC Experiments, Stockholm, Sweden, 10 - 14 Sep 2001, pp.325-330 (CERN-2001-005)

[20] J. R. Cook and G. Thomas, ELMB123 Documentation, https://edms.cern.ch/ui/file/684947/LAST_RELEASED/ElmbUserGuide.pdf

[21] P. Chochula *et al.*, The Evolution of The ALICE Detector Control System, Proceedings of ICALEPCS2015, Melbourne, Australia

[22] F. Costa, CRU Firmware Overview, The 7th ALICE ITS Upgrade, MFT, and O2 Asian Workshop, https://indico.cern.ch/event/484521/contributions/2239343/attachments/1316434/1972117/CRU_Firmware_Overview.pdf

[23] K. Wyllie *et al.*, A Gigabit Transceiver for Data Transmission in Future High Energy Physics Experiments, *Physics Procedia* 37 (2012) 1561

[24] GBT Project Team, GBTX Manual Draft V0.15, https://espace.cern.ch/GBT-Project/GBTX/Manuals/gbtxManual.pdf

[25] A. Caratelli *et al.*, The GBT-SCA, a radiation tolerant ASIC for detector control and monitoring applications in HEP experiments, *Journal of Instrumentation* 10 (2015) C03034

[26] K.M. Sielewicz et al., Prototype readout electronics for the upgraded ALICE Inner Tracking System, 2017 *JINST* 12 C01008

[27] R. Tieulent, MFT needs for detector tests, The 8th ALICE ITS Upgrade, MFT, and O2 Asian Workshop, https://indico.cern.ch/event/578890/contributions/2391065/attachments/1382606/2102600/Tieulent_MFT_O2_Needs.pdf

[28] CAEN, Technical Information Manual, http://www.caen.it/servlet/checkCaenManualFile?Id=10067